JOURNAL OF MATERIALS SCIENCE 20 (1985) 1341–1350

Environmental and time dependence of fracture toughness and crack growth in glass-fibre reinforced polyester resins

R. C. ROBERTS
Imperial Chemical Industries plc, Engineering Department, PO Box 7, Northwich, Cheshire, UK

The validity of simple (maximum load) fracture toughness testing of glass-fibre reinforced polyester resin laminates has been examined for SEN specimens using "slow strain rate" test techniques developed for metallic materials. Laminates were tested both in air and whilst immersed in an acidic environment. In general, valid test conditions were only established at test speeds $< 10^{-2}$ mm min^{-1} which are slower than those generally reported in the past. Fracture toughness was found to be greatly reduced by the presence of the chemical environment, as would be expected from the known sensitivity of these materials to environmental stress cracking. The slow strain rate test technique indicated a threshold level of critical stress intensity for environmental stress cracking and hence could be useful in ranking materials.

Environmental effects were also found to determine crack growth rates as measured on DCB specimens. Crack growth data was analysed in terms of initial and/or inherent flaws and its use in predicting creep-rupture life examined. In principle it was concluded that use of crack growth data could provide an alternative to the present qualitative approach to design and a more predictable alternative to long term creep-rupture testing.

1. Introduction

There is a recognized need [1] to design glass-fibre reinforced polyester (GRP) chemical process equipment on a more fundamental basis than the qualitative, experience-based approach embodied in current standards [2]. In some applications, the use of data [3] generated by testing laminates in air can be valid. This can be the case when a thermoplastic liner is specified, or when the failure mechanism involves mainly chemical degradation [4], and a "corrosion allowance", similar in concept to that applied to simple corrosion of metallic materials, is specified. In the majority of cases, however, the design must take into account the presence of a chemical environment in contact with the laminate. Failure is then by environmentally determined crack growth leading to the phenomena of environmental stress cracking (ESC) which has been found to occur under both static [1] and fatigue loadings [5]. In this case failure mechanisms involve environmental stress cracking of the reinforcing glass fibres and fracture surfaces are more characteristic of a brittle material showing a marked absence of fibre pull-out.

Factors affecting ESC such as resin matrix chemistry and glass-fibre type, content and orientation have now been extensively studied [6–8]. Progress has also been made [9, 10] in identifying glass fibres of different chemical composition to conventional E-glass, which, because of their greater resistance to chemical attack by acids and alkalis, can be used to manufacture composites having improved resistance to ESC.

In studies of fracture in air, in general it has been found difficult to establish valid conditions for fracture toughness testing [3]. However, because environmental stress failure occurs at much lower loads than observed in air and the fracture is more brittle, it might be expected that fracture mechanics could be more effectively

0022–2461/85 $03.00 + .12

applied to environmental crack growth. This has led to renewed interest [8, 10–12] in the application of fracture mechanics to crack growth in GRP in the presence of (particularly) acidic environments since the majority of applications for GRP vessels and pipework involve acidic contents.

In principle, data from short term crack growth studies can be used to predict lifetimes as a function of applied stress, as has been effectively demonstrated for high-density polyethylene [13]. For this material, creep-rupture life is determined by crack growth from very small inherent defects about 100 μm in size produced by the manufacturing process. The problem is more complex with GRP because whilst manufacturing defects can be much larger (millimetres in size) crack growth has been found to occur instead from smaller stress initiated micro-damage sites [5].

This paper describes a study of the effect of time and environment on simple fracture toughness tests on GRP from which it was hoped to provide a simple but quantitative criterion for resistance to environmental stress cracking which would have meaning in relation to service lives of decades. In addition, environmental crack growth rates have been determined on laminates reinforced with chopped strand mat, this type of reinforcement being chosen since it forms the basis of past and present successful process equipment and is used as the internal "chemical barrier" in the presence of other glass-fibre types such as woven or continuous rovings. The objective here was to examine the potential of crack growth data in predicting previously reported [1] long term creep-rupture data. Some data is also reported on laminates reinforced with glass-fibre woven rovings since these, together with glass-fibre continuous rovings are frequently incorporated within the structural part of laminates used in chemical process applications.

2. Experimental techniques

The resin used was ICI Atlac 385-05 bisphenol-fumarate polyester resin catalysed with 2 wt% benzolyl peroxide and 0.3 wt% demethylaniline accelerator. Plates 6 mm thick were hand laminated using either emulsion or powder bound chopped strand mat (TBA mat 77 or 80) or a balanced woven roving (TBA ECK 18), some samples having C-glass reinforced gel coats. The plates were lightly pressed in a closed steel mould using Melinex release film, and were cured in the moulds for 24 h at ambient temperature followed by post-curing for 3 h at 80° C. Samples were found to have glass contents of 31 wt% for chopped strand mat (CSM) reinforcement and 46 wt% for woven roving (WR) reinforcement. Test samples were cut from the plates using a diamond-impregnated slitting wheel.

Short term tensile properties were determined on 25 mm wide parallel edged samples using an Instron Model TT-DM; strain was determined using bonded strain gauges. For the CSM reinforced samples, the ultimate tensile strength, UTS, was 93 ± 5 MPa, ultimate tensile unit strength, UTUS, was 213 ± 9 MN mm^{-1} width per kg m^{-2} of reinforcement, tensile modulus, E, at 0.2% strain was 7500 ± 500 MPa and the unit tensile modulus, X, at 0.2% strain was 17 200 ± 1500 MN mm^{-1} width per kg m^{-2} of reinforcement. For the WR reinforced samples, UTS was 215 ± 15 MPa, UTUS was 290 ± 15 MN mm^{-1} width per kg m^{-2} of reinforcement, E at 0.2% strain was 14 000 ± 1000 MPa and X was 19 100 ± 1500 MN mm^{-1} width per kg m^{-2} of reinforcement.

Creep modulus at a stress of 15 MPa (for CSM samples) and 26 MPa (for WR samples) and relaxation modulus at a strain of 0.2% were determined on similar 50 mm wide samples on the Instron, strain measurements being made using bonded strain gauges. Under these conditions the two time dependent modulus values, $E(t)$, were found not to be significantly different. The values of $E(t)$ used for calculation of stress intensity during slow crack propagation were mean values of the experimentally determined creep and relaxation modulus (Fig. 1) which could be approximated for times to 10^6 sec by the equations

$$E(t) = 7650\, t^{-0.01122} \qquad \text{CSM laminates}$$

$$E(t) = 14\,100\, t^{-0.00872} \qquad \text{WR laminates.}$$

A critical stress intensity factor, K_c, was determined using single edge notch (SEN) specimens 25 mm wide. The variables studied included the ratio of notch depth, a, to sample width, w, notch tip radius of 0.15 and 0.9 mm, air or 5 wt% sulphuric acid environment and strain rate. Testing of samples immersed in acid was accomplished by cementing an acrylic tubular cell to the sample. Cross-head speeds (CHS) of 0.05 to 50 mm min^{-1} were obtained on the Instron whilst CHS down to 10^{-4} mm min^{-1} were obtained using a specially

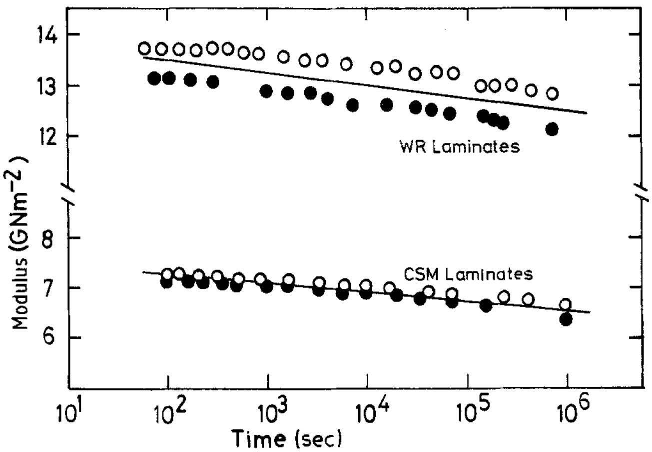

Figure 1 Creep (○) and relaxation (●) moduli of CSM and WR laminates.

built slow-strain tensometer. This was similar to that developed by Parkins [14] for stress-corrosion testing of steels. The cross-head was driven by a synchronous motor reduced up to $4 \times 10^6:1$ by three fixed and one variable gear train. Load was recorded from a strain gauge load transducer. During a typical test, load increased linearly with time until rapid crack propagation occurred. For this series of tests, K_c was defined in terms of the maximum load recorded, P_m:

$$K_c = Y\sigma(\pi a)^{1/2} = \frac{YP_m(\pi a)^{1/2}}{bw} \qquad (1)$$

where b is the sample thickness and the finite width K-calibration factor, Y, is given by Brown and Strawley [15] as

$$Y = 1.12 - 0.23\left(\frac{a}{w}\right) + 10.6\left(\frac{a}{w}\right)^2 - 21.7\left(\frac{a}{w}\right)^3 + 30.4\left(\frac{a}{w}\right)^4 \qquad (2)$$

Crack propagation tests were carried out using side grooved double cantilever beam (DCB) specimens. Most tests were done by application of a constant crack opening displacement rate using either the Instron or the slow-strain rig as appropriate. The very slowest crack speed determinations were done under load relaxation conditions. Tests were carried out both in air and the acidic environment using a clear PVC cell sealed to the tensometer grips to contain the acid. Because of possible local stress field variations by the presence of side grooves it was considered preferable not to use either a simple approximation [16] to K for this geometry:

$$K = 2\sqrt{3}\,\frac{Pa}{BH^{3/2}} \qquad (3)$$

or a more exact solution:

$$K = \frac{Pa}{B_c H^{3/2}}\left[3.46 + 2.3\left(\frac{H}{a}\right)\right] \qquad (4)$$

to calculate K and K_c. In preference the Irwin–Kies compliance relationship was used:

$$K = P\left(\frac{E}{2B_c}\frac{dC}{da}\right)^{1/2} \qquad (5)$$

where C is the compliance specific to the test sample and B_c the crack width. The compliance of several samples reinforced with each glass-fibre type was measured for a range of machined crack lengths, the results being shown in Figs. 2 and 3.

In order to use this data it is necessary to know the slope, dC/da as a function of either crack length or compliance. A range of standard computer curve fitting routines was investigated including polynomial, binomial, etc., but it was not found possible to accurately fit the C–a data over the whole range and obtain smooth dC/da data on differentiation. Our solution was to divide the compliance curve into some 16 spans and fit a cubic spline [17]. An explicit spline was used to fit a cubic polynomial of form

$$C = k_0 + k_1 a + k_2 a^2 + k_3 a^3 \qquad (6)$$

to each span, with end conditions for a Q-spline, two adjacent spans having a common end slope.

A further experimental difficulty was that it was not possible to define accurately the position of the growing crack tip, partially because of

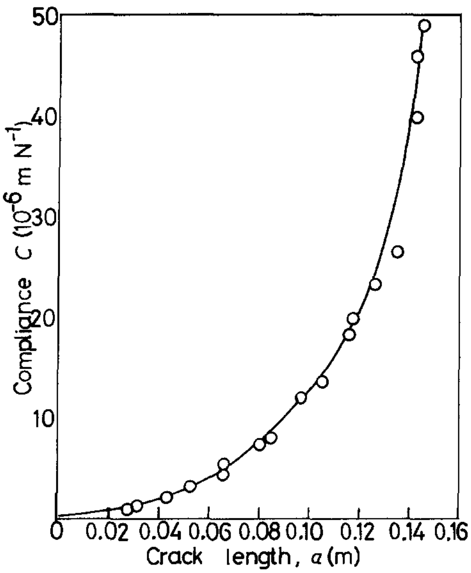

Figure 2 Compliance of CSM DCB test plates.

refractive index differences between resin and glass which led to poor translucency but largely because of the large damage zone at the crack tip. For this reason, apart from some optical measurements at the faster crack speeds, most determinations of crack length and hence growth rate were obtained indirectly from compliance measurements.

3. Results and discussion

3.1. Rising load determinations of K_c

3.1.1. Limitations to a simple experimental approach

Before discussing the experimental data it is illustrative to consider first of all the limitations

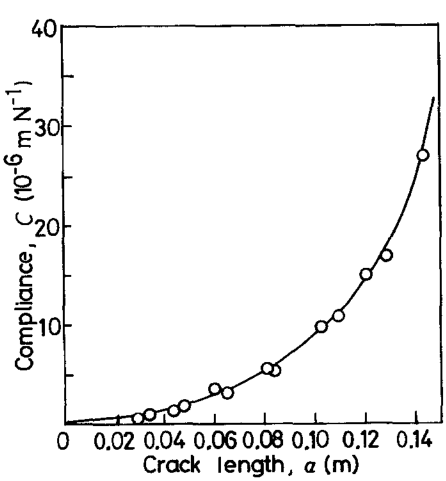

Figure 3 Compliance of WR DCB test plates.

[18] inherent in adopting the definition of K_c given by Equation 1. GRP materials do not yield but several microdamage processes do occur before failure and hence such processes will occur in the crack tip region. By analogy with plastic yield considerations (Irwin) the maximum plane stress radius of a zone of damage, r_d, is given by

$$r_d = \frac{1}{2\pi}\frac{K_c^2}{\sigma_d^2} \tag{7}$$

where σ_d is the stress causing damage. For a non-spherical damage zone, the size may be about 2.5 times greater (Dugdale model).

Using Equation 7 we can calculate r_d for the different values of K_c measured (see later), taking σ_d = 30% UTS which is the tensile stress at which matrix resin cracking may be detected audibly and the stress–strain curve becomes appreciably non-linear.

Considering the CSM laminates:

1. for $K_c = 10\,\text{MPa m}^{1/2}$ and $\sigma_d = 31\,\text{MPa}$, r_d = 16 mm;
2. for $K_c = 4\,\text{MPa m}^{1/2}$ and $\sigma_d = 31\,\text{MPa}$, r_d = 2.6 mm.

Considering the WR laminates:

1. for $K_c = 25\,\text{MPa m}^{1/2}$ and $\sigma_d = 72\,\text{MPa}$, r_d = 19 mm;
2. for $K_c = 5\,\text{MPa m}^{1/2}$ and $\sigma_d = 72\,\text{MPa}$, r_d = 0.8 mm.

Hence for plane stress testing, the effective crack length $(a + r_d)$, can be $\gg a$. For pure plane strain conditions, these values would be reduced by a factor of 9 but allowing for the existence of plane stress at the sample surface a more realistic correlation factor to apply to the above r_d values would be 3.

In order to ensure predominantly plane strain conditions in isotropic materials, sample thickness is often arbitrarily made greater than a minimum value B_{min} such that

$$B_{min} \geqslant \frac{2.5 K_c^2}{\sigma_y^2} \tag{8}$$

It is nevertheless illustrative to use Equation 8 to predict for the present planar isotropic CSM and orthotropic WR laminates the value of K_c for which plane strain will predominate for the 6.4 mm thick samples tested:

$$K_{c(crit)} \leqslant \left(\frac{6.4}{2500}\right)^{1/2} \sigma_d \tag{9}$$

1. For CSM samples $K_{c(crit)} \leqslant 1.6\,\text{MPa m}^{1/2}$;

2. For WR samples $K_{c(crit)} \leqslant 3.4\,\mathrm{MPa\,m^{1/2}}$.

The above considerations indicate that plane strain conditions were only approached for samples tested in the acidic environment and that all other values of K_c were obtained under conditions intermediate between plane stress and plane strain. Hence it is not surprising that K_c was found generally to be crack length dependent. Since the present study was aimed at determining values for $K_{c,\mathrm{ESC}}$ no attempt was made to correct for microdamage effects although it has been found [19] that crack length independent values of K_c could be obtained by taking $\sigma_d = 70\%\,\mathrm{UTS}$ for CSM laminates and $\sigma_d = 54\%\,\mathrm{UTS}$ for a balanced weave fabric reinforced laminate.

A further limitation of the rising load K_c data is imposed by use of the Strawley and Brown K-calibration function. Several authors [20] have shown that Y is also a function of the geometry of the reinforcement and that use of Y-values obtained for isotropic materials can lead to underestimation of K_c. Whilst the preferred experimental compliance calibration method was used for the crack growth study, no attempt was made to correct for sample anisotropy in the rising load K_c studies since the main objective was to investigate the usefulness of a simple experimental technique.

3.1.2. Experimental results

Values of critical stress intensity, K_c, calculated using Equations 1 and 2 are shown in Fig. 4 for CSM reinforced laminates. Samples were tested both in air and whilst immersed in 5 wt % sulphuric acid (without prior preconditioning in the environment). Cross-head speeds of 0.5 and 0.05 mm $\mathrm{min^{-1}}$ were investigated. All the results showed a good deal of scatter and the points shown are mean ± 1 standard deviation of some 5 individual measurements. There was little effect of notch tip radius from radii of 0.15 to 0.9 mm and hence the larger radius was generally used.

At CHS = 0.5 mm $\mathrm{min^{-1}}$ the results are crack length dependent and the presence of the acid significantly reduces K_c. At CHS = 0.05 mm $\mathrm{min^{-1}}$ the data is less crack length dependent and the K_c values of 4 to 5 $\mathrm{MPa\,m^{1/2}}$ are further reduced on average to some 50% of the values determined in air. The effect of CHS was further investigated at higher and lower speeds, the results being shown in Fig. 5 for samples with $a/w = 0.3$. K_c values approach limiting values for CHS $< 10^{-2}$

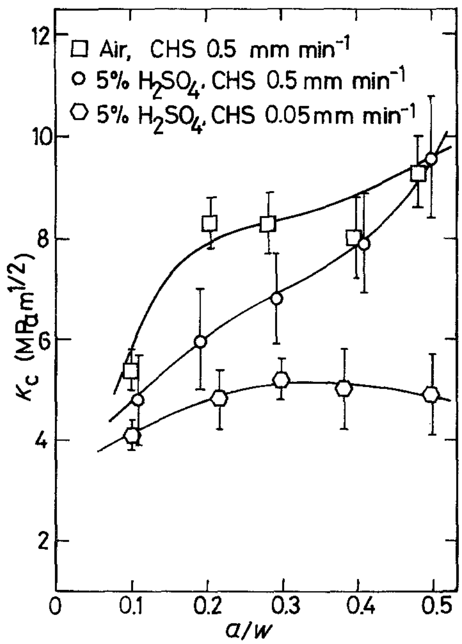

Figure 4 Fracture of CSM SEN laminates in air and 5% sulphuric acid.

mm $\mathrm{min^{-1}}$. The air value of 6.5 $\mathrm{MPa\,m^{1/2}}$ was reduced to $K_{c,\mathrm{ESC}} = 3.5\,\mathrm{MPa\,m^{1/2}}$ in 5% sulphuric acid. The shape of these curves show many similarities to stress corrosion cracking (SCC) curves [21] obtained for metallic materials such as chromium-nickel austenitic stainless steels and titanium

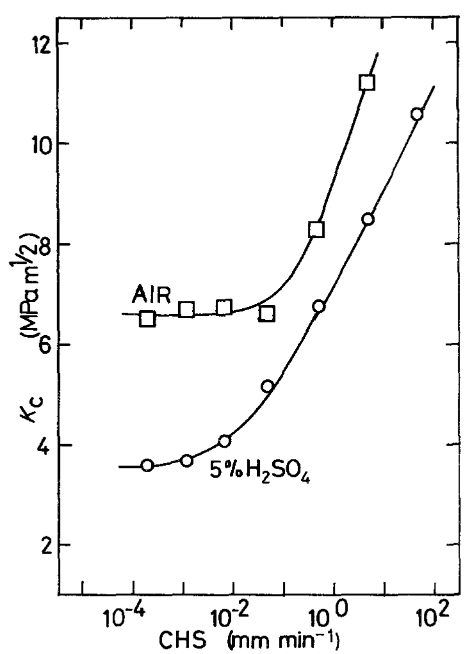

Figure 5 Effect of strain rate on fracture of CSM, SEN laminates in air and 5% sulphuric acid.

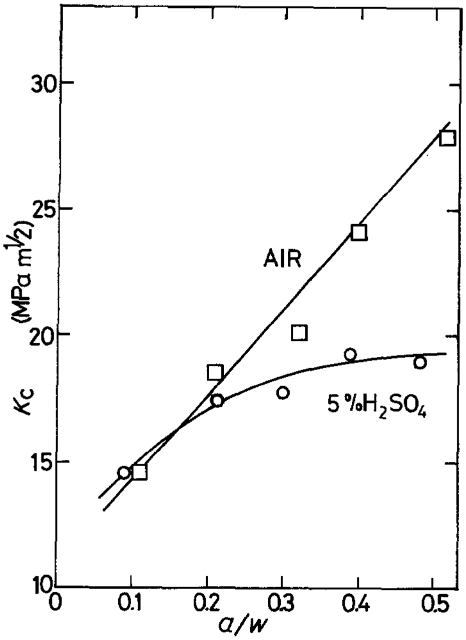

Figure 6 Fracture of WR, SEN laminates in air and 5% sulphuric acid.

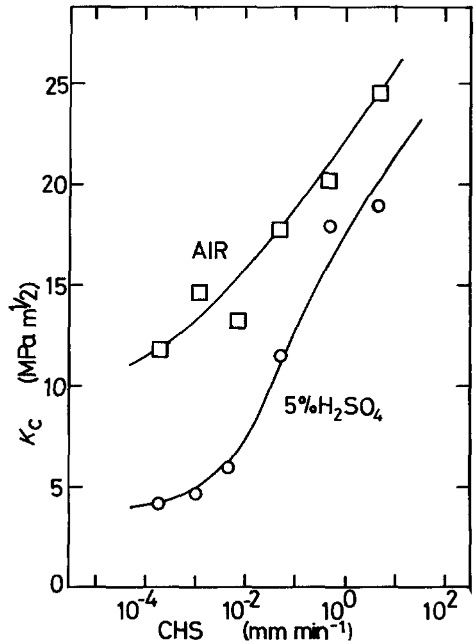

Figure 7 Effect of strain rate on fracture of WR, SEN laminates in air and 5% sulphuric acid.

alloys. For these metallic materials, the slow strain technique has been shown to correlate well with conventional constant load (time-to-failure) tests. Whilst the mechanisms of SCC of metals and ESC of plastics are quite different, in view of the simplicity of the slow strain technique, further measurements were made on woven roving laminates.

Fig. 6 shows K_c values calculated from Equations 1 and 2 and Fig. 7 shows the effect of strain rate on samples with $a/w = 0.3$. Here, again, there is evidence of an ESC limit and the values of $K_{c,ESC} = 4\,\mathrm{MPa\,m^{1/2}}$ in 5% sulphuric acid is not very different to the similar value for CSM laminates, but is significantly less than the values of more than $20\,\mathrm{MPa\,m^{1/2}}$ obtained in air at the higher strain rates.

3.2. Crack growth studies

There are two approaches (albeit very similar) to the analysis of crack growth data. Following the Paris fatigue crack growth relationship:

$$\frac{\mathrm{d}a}{\mathrm{d}N} = A\,\Delta K^n \tag{10}$$

crack growth under creep-rupture may be described by

$$\dot{a} = A' K_c^{n'} \tag{11}$$

where A, A', n and n' are constants. Whilst this expression more directly represents the fact that crack growth occurs as a result of an applied stress intensity, we prefer to write [22]

$$K_c = K_o(\dot{a}/\dot{a}_o)^m \tag{12}$$

where K_o and $\dot{a}_o$ are arbitrarily chosen reference constants which nevertheless can have practical significance if chosen as the lower limit to stress intensity and crack growth rate below which slow crack growth will not limit the use of the material. Neither of these relationships would be satisfactory if an ESC threshold were to exist.

On substitution from Equation 1:

$$K_o(\dot{a}/\dot{a}_o)^m = Y\sigma(\pi a)^{1/2}. \tag{13}$$

Failure will occur almost instantaneously by rapid crack propagation when $K_c = K_{Ic}$ the instability value of K_c. Hence the time-to-failure may be obtained by integration of Equation 13:

$$t = \frac{1}{\dot{a}_o}\left(\frac{K_o}{Y\sigma\pi^{1/2}}\right)^{1/m}\int_{a_o}^{a_c}\frac{\mathrm{d}a}{a^{1/2m}}$$

$$= \frac{1}{\dot{a}_o}\,\frac{2m}{1-2m}\left(\frac{K_o}{Y\sigma\pi^{1/2}}\right)^{1/m}$$

$$\times\left(a_o^{(2m-1)/2m} - a_c^{(2m-1)/2m}\right) \tag{14}$$

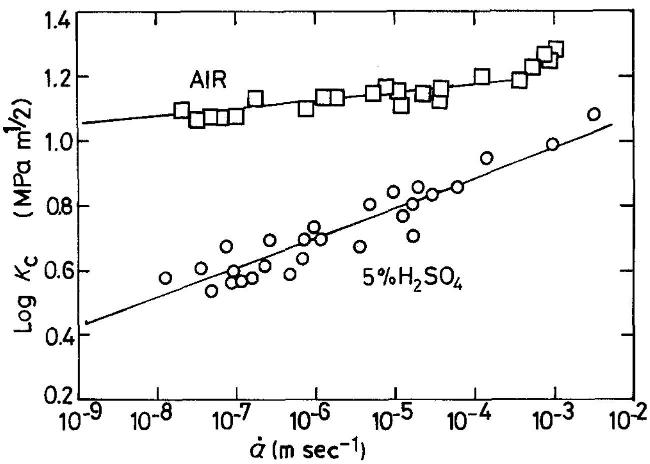

Figure 8 Crack growth data for CSM laminates in air and 5% sulphuric acid.

where a_o is the initial flaw size and a_c the critical flaw size given by

$$K_{Ic} = Y\sigma(\pi a_c)^{1/2} \quad (15)$$

noting that Y is also a function of a and sample geometry. For an uncracked sample, a_0 is the inherent flaw size and if this is $\ll a_c$ Equation 14 can reduce, for particular values of m, to

$$t = \frac{1}{\dot{a}_o}\frac{2m}{1-2m}\left(\frac{K_o}{Y\sigma\pi^{1/2}}\right)^{1/m} a_o^{(2m-1)/2m} \quad (16)$$

For many test samples it is found that Y is essentially constant for $a/w < 0.3$. Since it is crack growth in this range that determines time-to-failure, use of this approximation is justified.

Equation 16 has been used successfully to describe crack growth relationships for high-density polythene pipes [13, 22] and may be used in different ways. It can be used to determine the inherent flaw size, a_o of a laminate previously characterised by its crack growth and creep rupture behaviour. Having done this it can be used to predict times-to-failure as a function of applied stress for other environments for which K_o and m have been determined. Alternatively a practical value of a_o can be used based on damage levels set either by a subjective assessment of the likelihood of damage during service or by the lower limit to damage levels which can be monitored by non-destructive examination methods, such as ultrasonics.

Crack growth rates obtained for a wide range of applied K_c values (calculated from Equation 5) are shown for CSM reinforced laminates in Fig. 8 and WR reinforced laminates in Fig. 9. It can be seen that the crack growth data can be described quite well by Equation 12 with the following constants:

CSM laminates in air: $m = 0.025$. For $\dot{a}_o = 10^{-10}\,\mathrm{m\,sec^{-1}}, K_o = 10.5\,\mathrm{MPa\,m^{1/2}}$.

CSM laminates in 5% H_2SO_4: $m = 0.093$.

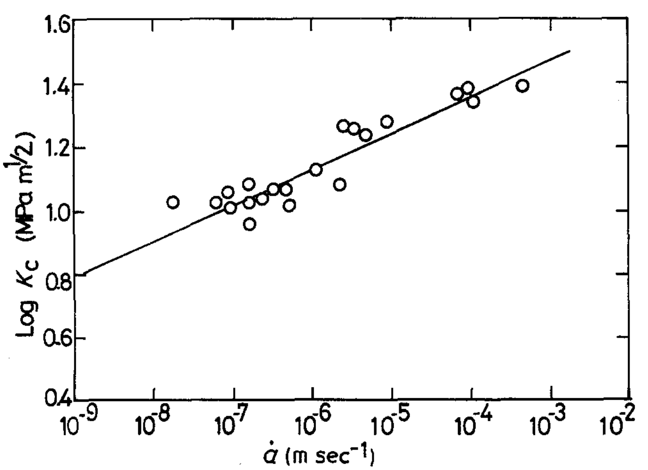

Figure 9 Crack growth data for WR laminates in 5% sulphuric acid.

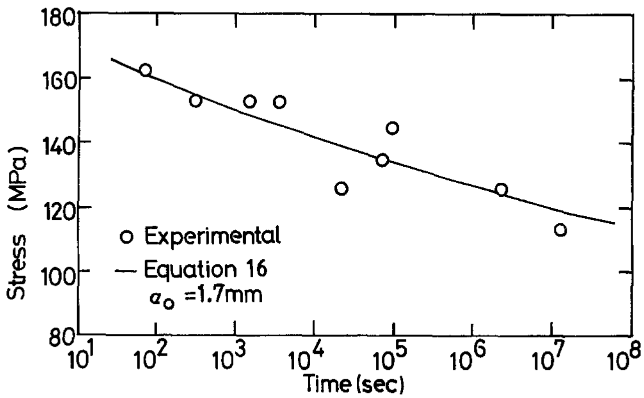

Figure 10 Creep-rupture data of CSM laminates in air. Solid line calculated from Equation 16 with $a_0 = 1.7$ mm.

For $\dot{a}_0 = 10^{-10}\,\text{m sec}^{-1}, K_0 = 2.1\,\text{MPa m}^{1/2}$.

WR laminates in 5% H_2SO_4: $m = 0.114$.

For $\dot{a}_0 = 10^{-10}\,\text{m sec}^{-1}$, $K_0 = 4.7\,\text{MPa m}^{1/2}$.

At a constant reference velocity of $10^{-10}\,\text{m sec}^{-1}$ ($\sim 3\,\text{mm year}^{-1}$), cracks would penetrate a vessel or pipe wall during its design lifetime, and hence cause leaks. Ultimately growth to a critical size to bring about catastrophic failure [23] would occur if remedial action were not taken. It is interesting to note that a stress intensity equal to K_0 would be present in a CSM plate when the maximum design strain [2] of 0.2% is applied, if there was present an edge crack of depth 5 mm (Equation 1, $Y = 1.12$).

Taking a reference velocity of $10^{-11}\,\text{m sec}^{-1}$, for laminates in 5% sulphuric acid, $K_0 = 1.72$ MPa $\text{m}^{1/2}$ and this level of stress intensity is similarly reached for an edge crack of depth about 3 mm. In practice, crack growth from such initial cracks would not occur at constant velocity but with velocity increasing with crack length. Equation 16 would predict lifetimes of 170 days and 4.4 years for initial defects of 5 and 3 mm respectively. Since these defect sizes are of the same order of magnitude as unavoidable air inclusions, which have been found not to be crack initiation sites, it would seem that use of non-destructive examination methods such as ultrasonics for flaw detection will not be straight-forward.

3.3. Creep rupture

In order to investigate possibilities for a design basis it is necessary to examine the ability of crack growth data to predict creep rupture behaviour. Fig. 10 shows previously published [1] creep rupture behaviour data on CSM laminates held in air under 3-point bending stress. The solid line was obtained from the K_c–$\dot{a}$ data using Equation 16. this best fit being obtained for an initial flaw size of 1.7 mm. Whilst at first sight this defect size would seem to be unrealistic it actually describes the failure process quite well. The CSM laminates suffered instantaneous macro gel coat and matrix resin cracking which penetrated the laminate when loaded to the stress levels of Fig. 10. The observed depth of these gel coat cracks was in the range 1 to 2 mm. Hence the initial defect size of 1.7 mm required by the fracture mechanics approach is not a true inherent defect but is the instantaneously produced initial crack. The K_c–$\dot{a}$ data then describe quite well the growth of this with time to bring about failure.

Fig. 11 shows creep rupture data [1] for CSM laminates under 3-point bending stress in 36 wt % hydrochloric acid and 36% hydrochloric acid/carbon tetrachloride mixtures for failure times now extended to over 10 years since several samples were retained on test after the original data were reported. It is illustrative to compare this data with the present crack growth data obtained for samples held in tension in 5% sulphuric acid. The justification for this is that the proposed [1] mechanism of environmental stress crack propagation involves attack by hydrogen ions, which both acids are able to provide, on glass-fibre surfaces.

In attempting to fit Equation 16 to this data it became clear that this could not be done using a unique value for a_0. If Y is given the value 1.12 [15], values of a_0 required to fit the smooth solid line in Fig. 11 can be calculated. These are shown as the broken line in Fig. 11. It would appear that two failure mechanisms are present. For high initially applied stresses, environmental crack growth data can describe the resulting short term failures, if there was present in the laminates a

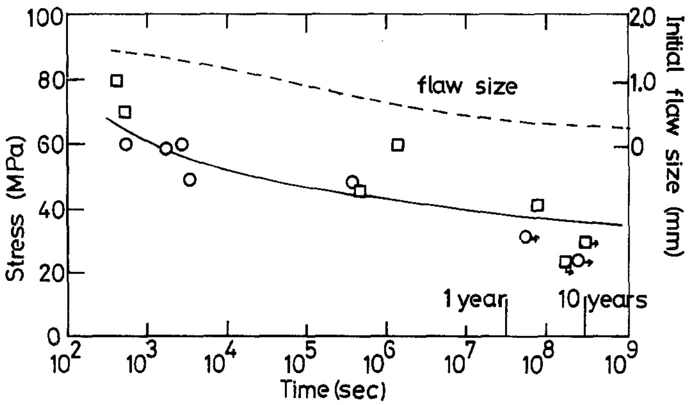

Figure 11 Creep-rupture data for CSM laminates in 36% hydrochloric acid (□) and 36% hydrochloric acid/carbon tetrachloride (○). Solid line is calculated from Equation 16 using a variable initial flaw size shown by the dotted line.

defect of size about 1.5 mm. For lower initially applied stresses, and hence design stresses, long term failure can be similarly explained by environmental crack growth from defects of size about 0.2 mm.

This model of defect size is in accordance with the known progressive and cumulative damage processes in CSM laminates under an increasing stress (see ref. [1] for earlier references), and proposed qualitative mechanisms for environmental stress failure [1, 5]. At low stresses the initial damage takes the form of matrix–fibre debonding within fibre bundles. The size of such damage zones has been measured by the author to be 0.1 to 0.5 mm. At higher stress levels these microcracks propagate into resin rich zones, can be visibly and audibly detected and those that penetrate the gel coat allow the environment access to exposed glass fibres. Their size is then 0.2 mm increasing to 2 mm at higher stresses. For the present creep rupture work, matrix resin cracking occurred almost instantaneously at bending stresses above 50 MPa thus explaining the high initial flaw size of about 1.5 mm predicted at these stresses and the lower initial flaw size required below this stress level. In this low-stress region it is probable that application of environmental K_c–$\dot{a}$ data alone is not valid since laminate life will be determined by an initial period of crack growth from an inherent defect until the environment gains access to exposed glass fibres. Crack growth from this stage will be more rapid and can be described by environmental K_c–$\dot{a}$ data. The present work does not allow this analysis to be done since we have not studied crack growth in air from inherent defects. Another area of uncertainty is the extent to which long term failure is initiated by diffusion of the environment into the laminate without prior microcracking as has been observed in uni-directional glass reinforced composites [7]. Also, whilst crack growth in the creep rupture work modelled through-wall crack growth in a vessel, the K_c–$\dot{a}$ data was obtained modelling edge crack growth in a plate. This is likely to be a second-order effect for the fibre orientations studied.

Fig. 12 shows creep rupture data for notched CSM laminates under 3-point bending stress in 36% hydrochloric acid. Samples were notched with a razor blade to a depth of about 0.4 mm such that the crack penetrated the gel coat and just entered the CSM reinforced laminate. The smooth solid line was calculated from Equation 16 using an initial defect size of 0.75 mm to obtain the best fit. Hence in this case also the K_c–$\dot{a}$ data is able to predict reasonably well the creep rupture data if we assume that the initial crack lengthened a small amount instantaneously on application of stress.

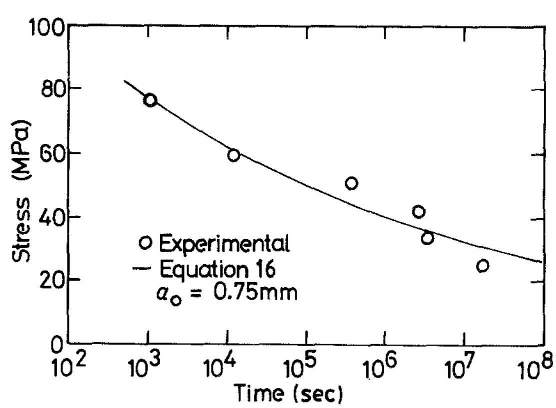

Figure 12 Creep-rupture data for notched CSM laminates in 36% hydrochloric acid. Solid line is calculated from Equation 16 with $a_0 = 0.75$ mm.

4. Conclusion

The determination of fracture toughness of GRP using slow strain techniques has illustrated the marked time dependance of such properties. Hence all such measurements should be quantified by details of the experimental time scale. When this is done, fracture toughness can be considered similarly to other time dependant properties such as modulus although the latter has a much smaller variation with time.

The fracture toughness of samples immersed in acids is about half that of similar samples tested in air. This is a consequence of acid induced environmental stress cracking. The slow strain techniques indicated limiting values for $K_{c,ESC}$ for CSM AND WR samples of 3.5 and 4.0 MPa $m^{1/2}$ respectively. These are similar to values recorded during very low-speed crack growth measurements. Hence slow strain fracture toughness testing would appear to have potential as a simple test for ranking materials in order of their ability to resist environmental stress-induced crack growth. Such data, however, is of limited use for design purposes.

Crack growth measurements, on the other hand, could provide a design basis by relating design stress to the stress required to grow a crack from an initial or inherent defect through the pipe or vessel wall during the design lifetime. In this study previously measured creep rupture lives of GRP immersed in acidic environments could be predicted from crack growth data making certain assumptions about growth mechanisms and initial defects. Further studies are needed to quantify crack growth in terms of glass-fibre type and orientation, resin type and pH and nature of environment. When this is done it should be possible to provide an alternative to the present qualitative approach to design.

Acknowledgement

The author acknowledges experimental assistance from W. S. Scurr and C. A. Hodgson and discussions with Dr J. G. Hines who provided computer software.

References

1. R. C. ROBERTS, *Reinf. Plast. Congr. (Brit. Plast. Federation)* (1978) 145.
2. BS 4994: 1973 (British Standards Institute, London).
3. M. J. OWEN, *Reinf. Plast. Congr. (Brit. Plast. Federation)* (1976) 167.
4. R. C. ROBERTS, GRP Vessels and Pipework for the Chemical and Process Industries, Symposium, UMIST, Manchester, 1983 (Mechanical Engineering Publications, London) p. 80.
5. W. S. CARSWELL and R. C. ROBERTS, *Composites* **11** (1980) 95.
6. F. R. JONES, J. W. ROCK and J. E. BAILEY, *J. Mater. Sci.* **18** (1983) 1059.
7. P. J. HOGG, D. HULL and B. SPENCER, *Composites* **12** (1981) 166.
8. G. P. MARSHALL and D. HARRISON, *Plast. Rubber. Process. Appl.* **2** (1982) 269.
9. S. TORP, S. OYSTEIN and M. ONARHEIM, 37th Annual Technical Conference, Reinforced Plastics/Composites Institute, (Society of the Plastics Industry, New York, 1982) Section 9E, p.1.
10. J. AVESTON and J. M. SILLWOOD, *J. Mater. Sci.* **17** (1982) 3491.
11. D. HULL and J. N. PRICE *ibid.* **18** (1983) 2798.
12. P. PRENTICE, J. C. RADON and C. WACHNICKI, *Plast. Rubber, Process Appl.* **3** (1983) 343.
13. A. GRAY, J. N. MALLISON and J. B. PRICE, *ibid.* **1** (1981) 51.
14. R. N. PARKINS, "Corrosion", Vol. 1 edited by L. L. Shreir, (Butterworths, London 1976) Chap. 8.10.
15. W. F. BROWN and J. E. STRAWLEY, ASTM STP 410 (1966).
16. G. P. MARSHALL, L. E. CULVER and J. G. WILLIAMS, *Plast. Poly.* **37** (February 1969) 75.
17. A. W. NUTBOURNE, R. B. MORRIS and C. M. HOLLINS, *Computer Aided Design* **45** (5) (1972) 228.
18. J. G. WILLIAMS, *Adv. Poly. Sci.* **27** (1978) 67.
19. M. J. OWEN and R. J. CANN, *J. Mater. Sci.* **14** (1979) 1982.
20. H. HAREL, G. MAROM, S. FISHER and I. ROMAN, *Composites* **11** (1980) 69.
21. H. BUHL, DFVLR Cologne Report No. DLR-FB 76–69 (1976).
22. J. G. WILLIAMS, Plasticon 81 Conference on Engineering Design with Plastics, University of Warwick, Sept. 1981, PRI (1981) p. 51.
23. R. C. ROBERTS, *Composites* **13** (1982) 389.

Received 16 February 1984
and accepted 4 June 1984